



## Observations of 1ES 0647+250 and 1ES 0806+524 with VERITAS

P. COGAN<sup>1</sup> FOR THE VERITAS COLLABORATION<sup>2</sup>.

<sup>1</sup>McGill University, 3600 University Street, Montreal, QC H3A 2T8, Canada

<sup>2</sup>For full author list see G. Maier, "Status and Performance of VERITAS", these proceedings  
coganp@hep.physics.mcgill.ca

**Abstract:** Observations of the blazars 1ES 0647+250 and 1ES 0806+524 with VERITAS are reported here. These objects are among the favoured candidate extragalactic sources in the very high-energy regime due to the presence of high-energy electrons and adequate seed photons. The presence of high-energy electrons is established from the location of the synchrotron peak in the spectral energy distribution of the blazars. The presence of adequate seed photons is determined by the flux in the radio-through-optical wavebands. These are the key ingredients for very high-energy gamma-ray emission in the context of the synchrotron self-Compton model. The redshift of 1ES 0647+250 has been tentatively reported as 0.203 and the redshift of 1ES 0806+524 is 0.138, thus the detection of very high-energy gamma-ray emission from these objects could make significant contributions to the understanding of the extragalactic infrared background light. The analysis of these data relies on standard techniques in very high-energy gamma-ray astronomy, and the results are compared to previously reported upper limits and to theoretical predictions.

## Introduction

The blazars 1ES 0647+250 and 1ES 0806+524 are among several blazars observed with VERITAS during its commissioning phase in late 2006 and early 2007. The observations of 1ES 0647+250 and 1ES 0806+524 are motivated by the search for very high-energy gamma-ray emission from extragalactic sources. In this paper two specific models used to predict VHE emission from blazars will be discussed and previously reported measurements and flux upper limits of the objects compared. The VERITAS instrument is briefly described and the results from the analysis of the VERITAS data are reported.

## Predictive Models

In the *modified-Fossati* model [1, 2], the peak frequency of the synchrotron spectrum and the relative importance of the inverse-Compton power are determined by the radio luminosity. The first modification assumes that objects of low power have equal luminosities in the synchrotron and self-

Compton components of their spectra. The second modification extends the radio range below  $10^{41.2} \text{ erg s}^{-1}$  by modeling Compton scattering in the Klein-Nishina regime. This modification also uses a different width for the parabola representing the Compton peak, which is reduced with respect to the synchrotron peak.

In the *Costamante* [1] model, a single zone SSC fit to multiwavelength data is used to predict fluxes in the TeV regime. The model emphasises the requirement of *both* high-energy electrons and sufficient seed photons to produce very high-energy gamma rays. In the study, a large sample of BL Lacs were examined and the radio/optical flux and synchrotron peak frequency fit using the SSC model. The flux predictions are summarised in Table 1.

Object	<i>Costamante</i>	<i>Modified-Fossati</i>
1ES 0647+250	0.59	0.24
1ES 0806+524	1.36	-

Table 1: Flux predictions according to the *Costamante* and *modified-Fossati* models. Fluxes are in units of  $10^{-11} \text{ cm}^{-2} \text{ s}^{-1}$  above 0.3 TeV.

## Targets

The blazar 1ES 0647+250 was discovered in the MHT-Green Bank survey at 5 GHz using the NRAO 91-m transit telescope. X-ray emission was discovered in the Einstein Slew Survey with the synchrotron peak falling just below 10 keV. A redshift of 0.203 has been tentatively reported. Previous observations of this object were reported by HEGRA [3] with a 99 % confidence flux upper limit of  $\mathcal{F}_{E>0.78 \text{ TeV}} < 33.5 \times 10^{-11} \text{ cm}^{-2} \text{ s}^{-1}$  from 4.1 hours of observations, where a spectral index of -2.5 was assumed. To compare this to the *Costamante* and *modified-Fossati* models, this can be extrapolated to  $\mathcal{F}_{E>0.3 \text{ TeV}} < 126.4 \times 10^{-11} \text{ cm}^{-2} \text{ s}^{-1}$  assuming a constant spectral index of -2.5 down to 0.3 TeV. This is well above both the predictions of the *Costamante* and *modified-Fossati* models and does not constrain either model.

The blazar 1ES 0806+524 was discovered using the NRAO Green Bank 91-m telescope at 4.85 GHz with X-ray emission reported by the Einstein Slew Survey. The galaxy has a measured redshift of 0.138. Whipple [4, 5] reported flux upper limits of  $\mathcal{F}_{E>0.3 \text{ TeV}} < 1.37 \times 10^{-11} \text{ cm}^{-2} \text{ s}^{-1}$ ,  $\mathcal{F}_{E>0.3 \text{ TeV}} < 16.80 \times 10^{-11} \text{ cm}^{-2} \text{ s}^{-1}$  and  $\mathcal{F}_{E>0.3 \text{ TeV}} < 1.47 \times 10^{-11} \text{ cm}^{-2} \text{ s}^{-1}$  from different observing seasons. HEGRA reported an upper limit of  $\mathcal{F}_{E>1.09 \text{ TeV}} < 42.5 \times 10^{-11} \text{ cm}^{-2} \text{ s}^{-1}$  in one hour of observations which can be extrapolated to  $\mathcal{F}_{E>0.3 \text{ TeV}} < 255.4 \times 10^{-11} \text{ cm}^{-2} \text{ s}^{-1}$  (assuming a spectral index of -2.5) to compare with the Whipple result and *Costamante* prediction. Neither the Whipple nor the HEGRA results constrain the *Costamante* model.

## Observations

All observations were taken in WOBBLE mode. In this mode, the target is offset from the center of the field of view by  $\pm 0.3^\circ$  or  $\pm 0.5^\circ$  in declination (or right ascension). One of the trade-offs with the WOBBLE mode is that although more time can be spent with the observational target in the field of view, the target is not at the center of the field of view where the sensitivity is highest. Thus the WOBBLE offset must be carefully chosen using

measurements or Monte Carlo simulations of the detector response to maximise sensitivity. All observations were taken during the VERITAS commissioning phase, where initially two telescopes and later three telescopes were complete. After selecting data to remove runs suffering from bad weather or technical problems, a total of 17.3 hours on 1ES 0647+250 and 34.7 hours on 1ES 0806+524 were available.

## Data Analysis

The data have been analysed using independent analysis packages (see [6] for details on the analysis package). All of these analyses yield consistent results. Standard data analysis techniques [7] for ground-based gamma-ray astronomy were used, and are briefly described here. The analysis was optimised using Crab Nebula [8] data from the same period.

Shower images in the focal plane are gain corrected and cleaned before being parameterised using a moment analysis. For each shower, the focal plane images are parameterised using Mean-Scaled Width and Length (MSW/MSL)[7]. These are calculated using a large data set of Monte Carlo simulations at discrete zenith ( $\Theta$ ) angles (with interpolation in  $\cos \Theta$ ). Cuts on MSL and MSW are designed to reject most of the background while retaining a large portion of the signal. The cuts for this analysis were optimised on a data set of Crab Nebula observations.

Background estimation is performed using the reflected-region background model. In this scheme, an integration region is placed around the putative source position, with identical background integration regions distributed around the field of view. The number of events in the integration region is termed  $On$ , the number of events in the background region is termed  $Off$  and the ratio of the integration areas is termed  $\alpha$ .

The analysis results are summarised in Table 2, with the data from both objects broken down in terms of the number of participating telescopes. The statistical excess is calculated using equation 17 from [9]. No excess above  $5\sigma$  is uncovered in any of the data. A distribution of  $\theta^2$  for the signal and background regions for both sources is

shown in Figures 1 and 2. The  $\theta^2$  distribution shows the squared angular distance between the putative source position and reconstructed shower source. The red line marks the  $\theta^2$  distribution relative to the putative source position and the blue points mark the averaged  $\theta^2$  distribution relative to the background positions. The signal integration region is to the left of the vertical line.

In the absence of a clear signal greater than  $5\sigma$ , upper limits for both objects can be derived. This is done in order to compare the predictions of the *Costamante* and *modified-Fossati* models and to previous reports. The upper limit is found from the probability density function of the number of counts from the putative source [10].

$$p I\left(\frac{-C}{\sigma}\right) = I\left(\frac{C^{\text{UL}} - C}{\sigma}\right) \quad (1)$$

where  $p$  is the confidence level,  $C$  is the number of excess counts,  $\sigma$  is given by

$$\sigma = \sqrt{on + \alpha^2 Off} \quad (2)$$

and the function  $I$  is given by

$$I(z) = \frac{1}{\sqrt{2\pi}} \int_z^\infty e^{-x^2/2} dx \quad (3)$$

The energy threshold (peak energy response after gamma-ray selection cuts) for each data set is calculated using a data base of Monte Carlo gamma-ray simulations at multiple zenith angles. The energy threshold is found by interpolation in  $\cos\Theta$  using the mean elevation of each data set.

After calculating the 99% upper limit on the number of counts. It is then expressed in terms of Crab Nebula units, and converted into a flux upper limit by scaling relative to the Crab Nebula flux. These results are shown in Table 2. The differential flux upper limits are shown in Figure 3.

## Discussion

The upper limits calculated for 1ES 0647+250 are significantly better than those reported previously. The *Costamante* model is surpassed, however with an extremely low prediction of  $\mathcal{F}_{E>0.3 \text{ TeV}} =$

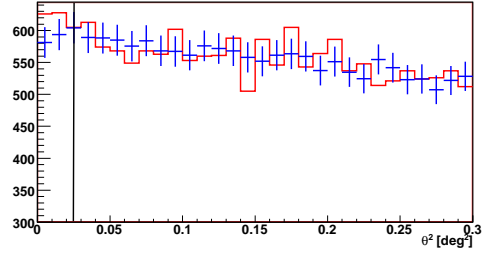


Figure 1:  $\theta^2$  distribution for 1ES 0647+250 - the signal integration region is to the left of the vertical line. The background counts are given by the crosses.

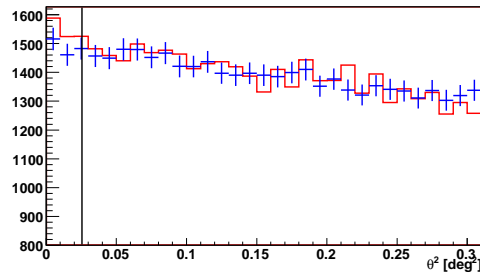


Figure 2:  $\theta^2$  distribution for 1ES 0806+524 - the signal integration region is to the left of the vertical line. The background counts are given by the crosses.

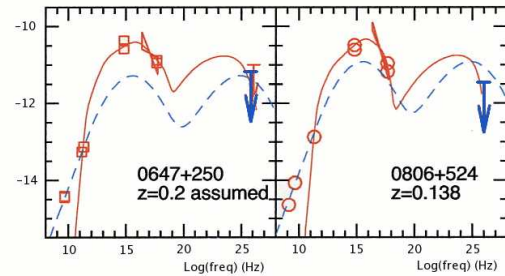


Figure 3: Spectral energy distributions of 1ES 0647+250 and 1ES 0806+524 from [1], with the differential flux upper limits from this work overlaid in blue. The vertical axis displays  $\log(vFv)$  in units of  $\text{erg cm}^{-2} \text{s}^{-1}$ .

Target	Data Set	Exposure (hrs)	Excess	$\sigma$	$E_{\text{th}}^{\text{TeV}}$	$\mathcal{F}_{E>0.3\text{TeV}}^{\text{UL}}$
1ES 0647+250	2-Tel	16	38	1.5	0.275	0.58
1ES 0647+250	3-Tel	1.3	13	2.1	0.225	1.3
1ES 0647+250	<i>All</i>	17.3	51	2.0	0.275	0.62
1ES 0806+524	2-Tel	8.5	18	1.3	0.345	0.42
1ES 0806+524	3-Tel	26.2	67	2.1	0.36	0.15
1ES 0806+524	<i>All</i>	34.7	85	2.5	0.36	0.13

Table 2: Summary of the VERITAS observations of 1ES 0647+250 and 1ES 0806+524 from November 2006 to March 2007. The data are categorised in terms of the array configuration. The energy threshold,  $E_{\text{th}}^{\text{TeV}}$ , is calculated for the average zenith angle of the dataset in TeV. The Excess is  $On - \alpha Off$  and  $\sigma$  is the statistical significance as calculated using Equation 17 from [9].  $\mathcal{F}_{E>0.3\text{TeV}}^{\text{UL}}$  is the flux upper limit above 0.3 TeV in units of  $10^{-11} \text{ cm}^{-2} \text{ s}^{-1}$ .

$0.24 \times 10^{-11} \text{ cm}^{-2} \text{ s}^{-1}$ , the *modified-Fossati* prediction is not surpassed. The upper limits calculated for 1ES 0806+524 are also significantly better than those reported before, and surpass the *Costamante* model.

Although predictions for the *Costamante* model on both objects are surpassed, the implications are not necessarily severe for SSC modeling, especially given the uncertainties in scaling of flux limits when the spectrum is unknown. The prediction of TeV fluxes is extremely sensitive to small variations in model parameters such as radio and X-ray flux. Also, the flux predictions were built from multiwavelength data on sources that are known to exhibit variability. Thus the flux at the lower energy regions of the data sets may have been different during these VERITAS observations, than it was when the multiwavelength data from which the model was built.

Given the lack of detectable quiescent emission with a modestly deep exposure, these objects are unlikely to be the subject of future deep observations with an instrument of this class. However, given that optical and x-ray flaring have been linked to detectable increases in emission in the TeV regime, future campaigns may revolve around target-of-opportunity triggers from the multiwavelength community.

## Conclusions

No evidence for emission is found from observations of 1ES 0647+250 and 1ES 0806+524. Con-

straining upper limits were placed on the emission from 1ES 0806+524 in the TeV regime. The VERITAS blazar key science project promises exciting results in the future as the array reaches maturity.

## Acknowledgements

This research is supported by grants from the U.S. Department of Energy, the U.S. National Science Foundation, the Smithsonian Institution, by NSERC in Canada, by Science Foundation Ireland and by PPARC in the UK.

## References

- [1] L. Costamante, G. Ghisellini, AAP 384 (2002) 56–71.
- [2] G. Fossati, MNRAS 299 (1998) 433–448.
- [3] F. Aharonian, AAP 421 (2004) 529–537.
- [4] D. Horan, APJ 603 (2004) 51–61.
- [5] I. de la Calle Pérez, APJ 599 (2003) 909–917.
- [6] P. Cogan, These Proceedings.
- [7] M. Daniel, These Proceedings.
- [8] O. Celick, These Proceedings.
- [9] T.-P. Li, Y.-Q. Ma, APJ 272 (1983) 317–324.
- [10] O. Helene, NIM 212 (1983) 319.